STRUCTURAL BEHAVIOR OF THE HYBRID COMBINATION OF CFRP-BFRP SHEETS IN RETROFITTING OF RC BEAMS BASED ON NONLINEAR FINITE ELEMENT ANALYSIS

Ibrahim Mohamed Metwally*

Concrete Structures Research Institute, Housing & Building Research Centre, P.O. Box 1770 Cairo, Egypt

Corresponding Author: ibrahimhbrc@gmail.com

Abstract: The use of composite materials such as fiber-reinforced polymers in strengthening and repairing of reinforced concrete elements is widely spreading. However, for successful and cost-effective applications, engineers must improve their knowledge with respect to the actual behavior of strengthened structures. The CFRP sheets used in strengthening applications have high strength; however, they are brittle materials with low ductility. Basalt fiber reinforced polymer (BFRP) sheets on the other hand have relatively lower strength compared to CFRP, however they have higher ductility and cheaper than carbon fibers. As a result, there is growing interest among researchers and practitioners in combining different types of FRP sheets to produce an enhanced strengthening system in terms of strength and ductility. This hybrid system is designed to enhance the properties of composites, where it combines the high strength of CFRP and high ductility of BFRP sheets, respectively. This paper presents the nonlinear finite element analysis (FEA) that has been carried out to simulate the behavior of failure modes of reinforced concrete (RC) beams strengthened in flexure using CFRP sheets, BFRP sheets, and their hybrid combination (CFRP-BFRP). Besides, new technical approach is presented numerically to show that concrete cover replacement with high strength concrete one provided better load capacity and failure mode, indicating utmost utilize of the hybrid combination of CFRP-BFRP in strengthening of RC beams. The commercial and general finite element analysis; ABAQUS software is used for modeling and nonlinear analysis. Load deflection relationships, failure mode, ductility, ultimate load and ultimate deflection were obtained and compared with the recent experimental results available in literature. From the analysis, it is found that FEA can predict accurately the load-displacement relation and good agreements were obtained when compared to the experimental data. In addition, the proposed FE analysis can be reliably used as a cost-effective tool to predict the inelastic behavior of strengthened beams.

Keywords: *RC beams, strengthening, CFRP, BFRP, nonlinear, FEA*

1.0   Introduction

Carbon fiber reinforced polymer (CFEP), glass fiber reinforced polymer (GFRP), aramid fiber reinforced polymer (AFRP) and basalt fiber reinforced polymer (BFRP) are four materials suitable for strengthening concrete structures. In this study, the author concentrates only the CFRP and BFRP and their combinations. CFRP is a very strong and light composite material, which consists of carbon fibers embedded in a thermosetting resin known as the matrix. This high performance material has been widely used due to its various advantages. It has a very high modulus of elasticity, high tensile strength, low density, good corrosion resistance, low coefficient of thermal expansion, and high chemical inertness. Yet, CFRP sheets are relatively expensive, have high electric conductivity, and fail in a brittle manner (Choobbor *et al*., 2014). Ashour *et al. (*2004) and Ahmad & Sobuz *(*2011) they tested many RC members to evaluate the flexural performance of RC beams strengthened with CFRP sheets with different arrangement schemes. They reported that CFRP strengthening has greatly improved the load carrying capacity of reinforced concrete beams. Moreover, they revealed that increasing the number of CFRP laminate layers increases the flexural stiffness, yield load, and ultimate load. In addition, they observed that no inter-layer delamination occurred; rather the strengthened beams failed suddenly in a brittle manner, where the concrete cover adjacent to the CFRP sheets peeled suddenly.

Sveinsdóttir (2012) reported in his dissertation that BFRP has been increasingly used in many applications for its numerous advantages such as resistance to high temperature, durability, and resistance to chemicals and alkaline. Besides, BFRP has several advanced properties making it a very favorable material in structural applications. BFRP has a similar coefficient of thermal expansion as concrete, natural resistance to corrosion, alkali, and acids, and does not absorb or transfer moisture like GFRP. Furthermore, BFRP laminates are remarkable in terms of fire resistance, which make them emerge as a strong alternative to other types of FRP composites. BFRP is cheaper and has a relatively large elongation. However, the elastic modulus of BFRP is significantly lower than that of carbon fiber. As a result, the ductility and stiffness of CFRP-strengthened beams are noticeably lower and higher than those of BFRP- strengthened beams respectively. In order to use fiber materials more efficiently, it is a requirement to increase the elongation with a slight influence on stiffness.

Choobbor *et al*. (2014) proposed an idea to strengthen reinforced concrete beams by combining CFRP and BFRP sheets. On the other hand, the hybrid CFRP-GFRP strengthening systems have been used extensively and are proven effective in increasing both strength and ductility as recommended by Xiong *et al*. (2004); Kim *et al. (*2011); Grace *et al*. (2002); Wu *et al*. (2006); Choi *et al*. (2011) and Hawileh *et al*. (2014). However, the hybrid CFRP- BFRP strengthening system has not been studied enough until now; very few research works is present in the literature. Therefore, the importance of this investigation becomes evident to contribute to this missing body of knowledge

(experimentally and numerically) and introduce the deep understanding of this technique. The FE results were validated against experimental data obtained from Choobbor *et al*. (2014). In addition, a new approach was evaluated based on FE analysis for obtaining the best flexural performance of the hybrid CFRP- BFRP strengthening technique.

2.0   Experimental Technique

The results of the experimental work of retrofitted RC beams which recently was done by Choobbor *et al*. (2014) were used for comparison and verification of the finite element analysis. Hence, the finite element model was implemented based on the parameters and conditions in the laboratory tests made by Choobbor *et al*. (2014). Eight RC beams, one was control (unstrengthened beam) and others were strengthened with CFRP, BFRP, and their different hybrid combinations. All tested beams have the same geometry. The details, geometry, and reinforcement of the specimen are shown in Figure 1. All beams were simply supported and tested under four point bending until failure. Universal testing machine, with a hydraulic actuator and a maximum capacity of 2500kN, was used to apply a monotonic load and simulate a static loading condition. Flexural tests were displacement controlled with a rate of 2 mm/min applied on the mid-span of the RC beams. The loading and the vertical deflection readings were recorded after every load increment besides modes of failures were captured. Test setup is shown in Figure 2.
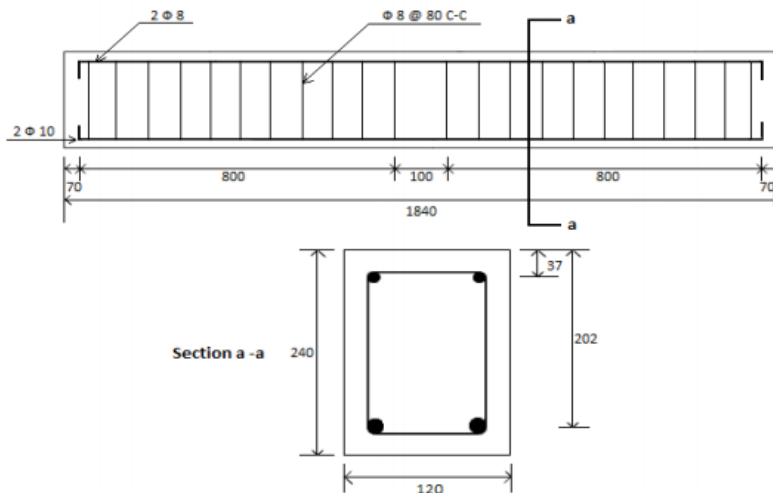
Figure1: Specimen dimensions and details(mm)
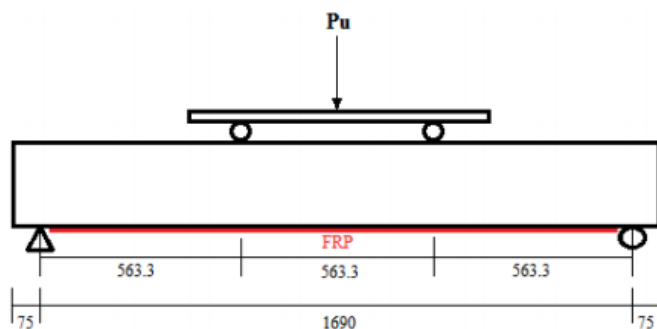
Figure 2: Schematic of flexural test set-up (mm)

All FRP sheets used for strengthening covered the full width of the RC beams and 90% of the RC beams' length with dimensions of 120mm x 1520mm. Table 1 lists all RC beams tested by Choobbor *et al*. (2014). Beams strengthened with FRP sheets are denoted with C and B, referring to CFRP and BFRP laminates, respectively.

Table 1: Strengthening scheme of specimens

Specimen	Number of FRP layers	Strengthening type
NS	0	No Strengthening
C	1	One layer of CFRP
CC	2	Two layer of CFRP
B	1	One layer of BFRP
BB	2	Two layer of BFRP
BC	2	One layer of BFRP bonded with one layer of CFRP
BCC	3	One layer of BFRP with two layers of CFRP ; bonded in sequence
BCB	3	One layer of BFRP, one layer of CFRP and one layer of BFRP; bonded in sequence

3.0   Finite Element Analysis using ABAQUS

The finite element analysis package ABAQUS/Standard (2016) was used for modeling the retrofitted RC beams. Brief descriptions for the constitutive models that are used in the model are described below:

3.1   Material Properties and Constitutive Models

3.1.1   Concrete

A concrete damage plasticity model available in ABAQUS was used to model the concrete behavior. This model assumes that the main two failure modes are tensile cracking and compressive crushing as recommended by ABAQUS/Standard (2016). To specify the post-peak tension failure behavior of concrete the fracture energy method was used according to Hillerborg (1985). The fracture energy (G_f) is the area under the softening curve and was assumed equal to 0.14 N/mm, as presented in Table 2. The stress–strain relationship proposed by Saenz (1964) was used to construct the uni-axial compressive stress–strain curve for concrete. The Young's modulus and tensile strength of concrete were calculated based on ACI 318-14(2014) as shown in Table 2.

3.1.2   Steel Reinforcement

The material properties assigned to the steel reinforcement were obtained from the experimental results of Choobbor *et al*. (2014). The nonlinear behavior of longitudinal steel bars and stirrups were modeled in ABAQUS based on the stress- strain curve with strain hardening as shown in Table 3.

3.1.3   FRP Laminates

The CFRP, BFRP, and their combinations were considered as a linear elastic orthotropic material until failure. The used FRP laminates are orthotropic materials, which mean they have different mechanical properties along different directions. The composites are unidirectional and their material properties in the x direction (fiber direction) were obtained from coupon tests as tested by Choobbor *et al*. (2014). Coupon laminates consist of FRP sheets impregnated with an epoxy resin. The used adhesive was Sikadur-330, a 2-part epoxy resin, was used to attach FRP sheets to the tension face of concrete beams. The manufacturer specifies a tensile strength, flexural elastic modulus, and tensile elastic modulus of 30 MPa, 3800 MPa, and 4500 MPa, respectively for the used adhesive. The mechanical properties of FRP materials in the y and z directions (perpendicular to the fiber direction) were also defined. Table 4 summarizes the mechanical properties assigned to the FRP composites coupons. Moreover, due to some specimens failing by BFRP rupture, damage and failure of the BFRP sheet and other FRP-composites were numerically simulated by adopting the Hashin model, which is incorporated in ABAQUS/Standard (2016).

Table 2: Concrete properties

Elastic properties	$E_C = 4700\sqrt{f_c} = 29725$ MPa	
	Poisson's ratio = 0.15	
Plastic properties	Ultimate compressive strength (f''_c) = 40 MPa	
	Ultimate compressive strain = 0.0025	
	Tensile strength (f_{ct}) $=0.35\sqrt{f_c}$ =2.2MPa	
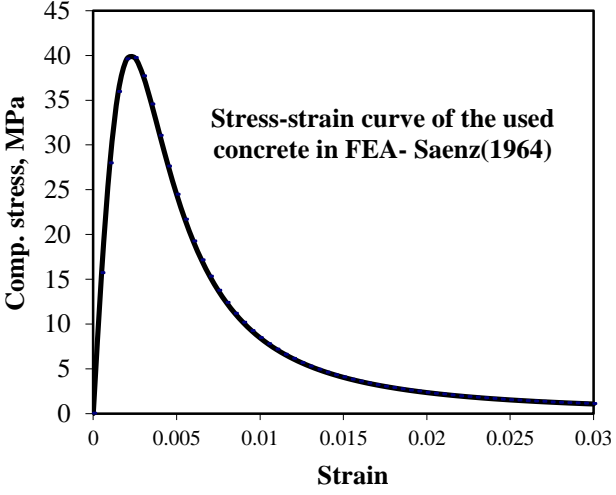
Stress-strain curve of the used concrete in FEA- Saenz(1964)
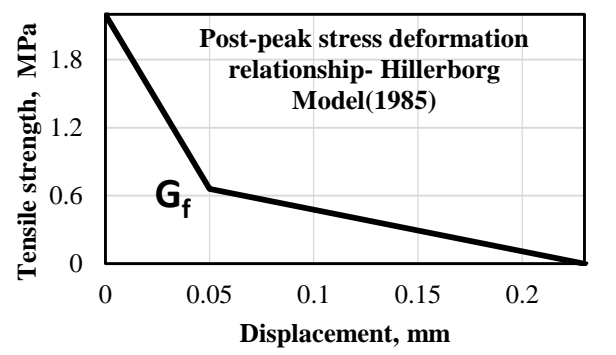
Post-peak stress deformation relationship- Hillerborg Model(1985)

G_f

Table 3 : Experimental properties of steel reinforcement

Elastic properties	E=199970MPa
	Poisson's ratio = 0.3
Plastic properties	Yield stress= 540.14 MPa
	Ultimate stress = 640.17 MPa

Experimetal stress-strain curve of steel bars used in FEA

(Stress, MPa vs Strain)

Table 4 : Experimental properties of FRP coupon laminates

Specimen	Thickness mm	E_x GPa	$E_y=E_z$ GPa	$v_{xy}=v_{xz}$	v_{yz}	$G_{xy}=G_{xz}$ GPa	G_{yz} GPa	Tensile strength MPa	Ult. tensile strain
C	0.63	49.94	3.5	0.28	0.42	1.37	1.23	781.91	0.0174
CC	1.24	46.05	3.22	0.28	0.42	1.26	1.14	706.50	0.0177
B	0.72	17.79	1.25	0.15	0.21	0.54	0.52	411.27	0.0232
BB	1.03	24.98	1.75	0.15	0.21	0.76	0.72	489.04	0.0259
BC	1.03	45.67	3.2	0.22	0.32	1.31	1.21	770.01	0.0202
BCC	1.59	38.91`	2.72	0.24	0.35	1.01	1.01	758.63	0.0246
BCB	1.61	37.81	2.65	0.19	0.28	1.11	1.03	704.02	0.0208

3.1.4 FRP-Concrete Interface

The FRP-concrete interface was modeled using ABAQUS surface-based cohesive behavior based on a traction-separation law. Figure 3 shows a graphic interpretation of a simple bilinear traction-separation law written in terms of the effective traction, τ, and effective opening displacement, δ. Obaidat *et al. (*2010) suggested that the interface is modeled as a rich zone of small thickness with an initial stiffness, K_0, defined as:

$$K_0 = \frac{1}{\frac{t_i}{G_i}+\frac{t_c}{G_c}}$$
(1)

Where t_i is the adhesive thickness, t_c is the concrete thickness, and G_i and G_c are the shear modulus of adhesive resin and concrete, respectively. The values used for this study were $t_i = 1$ mm, $t_c = 5$ mm, $G_i = 1.73$ GPa, and $G_c = 12.4$ GPa.
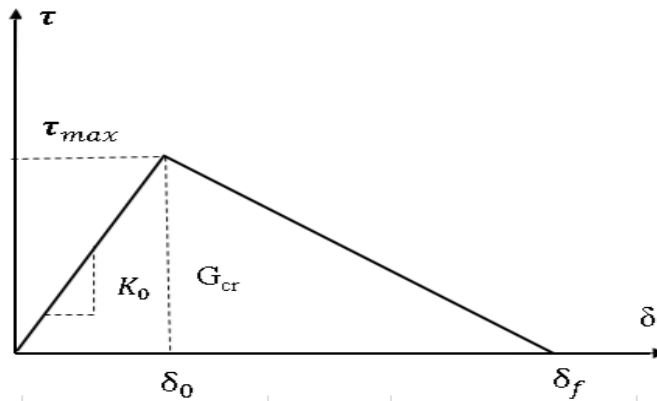
Figure 3: Bilinear traction–separation constitutive law

The maximum bond shear stress, τ_{max}, was computed according to Eq. 2. It provides an upper limit for the maximum shear stress, τ_{max} as recommended by Obaidat *et al. (*2010):

$$\tau_{max} = 1.5\, \beta_w f_{ct} \tag{2}$$

Where

$$\beta_w = \sqrt{\left(2.25 - \frac{b_f}{b_c}\right) / \left(1.25 + \frac{b_f}{b_c}\right)}$$

and b_f is CFRP plate width, b_c is concrete width and f_{ct} is concrete tensile strength. The value of τ_{max} which computed by Eq.2 is always too high as stated in the dissertation of Obaidat (2011) (in this case $\tau_{max} = 2.46$ MPa) ; it was reduced to 1.5 MPa to obtain the realistic results. The fracture energy, $G_{cr} = 0.09$ mJ/mm^2 was also used as recommended by Obaidat *et al. (*2010).

The initiation of damage was assumed to occur when a quadratic traction function involving the nominal stress ratios reached unity. This criterion can be represented as described by Obaidat *et al. (*2010):

$$\left\{\frac{\sigma_n}{\sigma_n^0}\right\}^2 + \left\{\frac{\tau_s}{\tau_s^0}\right\}^2 + \left\{\frac{\tau_t}{\tau_t^0}\right\}^2 = 1 \qquad (3)$$

Where σ_n is the cohesive tension and τ_s and τ_t are shear stresses at the interface, in which *n, s,* and *t* refer to the direction of the stress component. The values used for this simulation were $\sigma_n^0 = f_{ct} = 2.2$ MPa, and $\tau_s^0 = \tau_t^0 = 1.5$ MPa. Interface damage evolution was expressed in terms of energy release. The description of this model is available in the ABAQUS/Standard (2016) material library. The dependence of the fracture energy on the mode mix as defined by ABAQUS/Standard (2016) based on the Benzaggah–Kenane fracture criterion as follows:

$$G_n^c + (G_s^c - G_n^c)\left(\frac{G_\varphi}{G_j}\right)^\eta = G^c \qquad (4)$$

where $G_\varphi = G_s + G_t$; $G_J = G_n + G_s$; and η is the material parameter. G_n, G_s and G_t refer to the work done by the traction and its conjugate separation in the normal, first and the second shear directions, respectively. The values used for this study were $G_n^c = 0.09$ mJ/mm^2, $G_s^c = G_t^c = 0.9$ mJ/mm^2, and $\eta = 1.45$.

3.2 Boundary Conditions

One quarter of the specimen was modelled by taking advantage of the double symmetry of the beam in three- dimensions (Figure 4). Load was applied in the form of an imposed displacement. A displacement-controlled load was selected for the analysis to capture the response of the beam beyond its peak load. A pin-support was used to restrain the beam in the vertical direction.
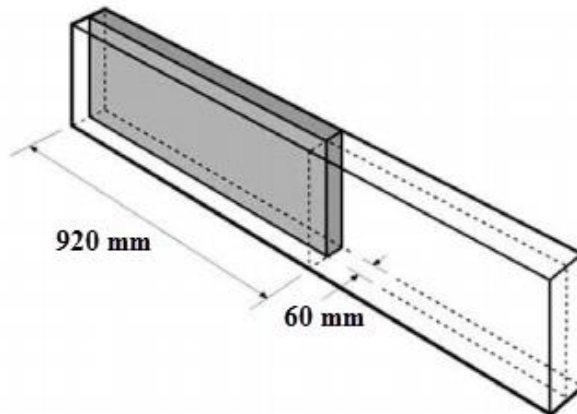
Figure 4: Model of one quarter of the beam

3.3   *Element and Mesh Sensitivity*

Eight-node brick elements with reduced integration (C3D8R) were adopted for simulation of the concrete beam, loading and bearing plates, whilst the longitudinal reinforcing bars and the steel stirrups were molded with two-node truss elements(T3D2) embedded in the concrete region (i.e. no relative displacement between reinforcement and concrete was allowed). Four-node shell elements with reduced integration (S4R) were used to model the FRP sheets**.** To verify the FE analysis and mesh sensitivity, four different mesh sizes were selected for the simulation of the un-strengthened beam (control) as shown in Figure5 (a).

The results were compared with the measured load-deflection curve, and FE models with the different mesh sizes were found to represent the behavior of RC beam well as shown in Figure5(b). Fine (20x20x20 mm) and very fine meshes (10x10x10 mm) give bad simulations as shown in Figure 5(b). On the other side, coarse (40x40x40 mm) and medium meshes (30x30x30 mm) attained nearly the same behavior. Therefore, medium mesh (30x30x30 mm) in Figure5 (a) was selected for the rest of the simulations because it gives more realistic behavior.
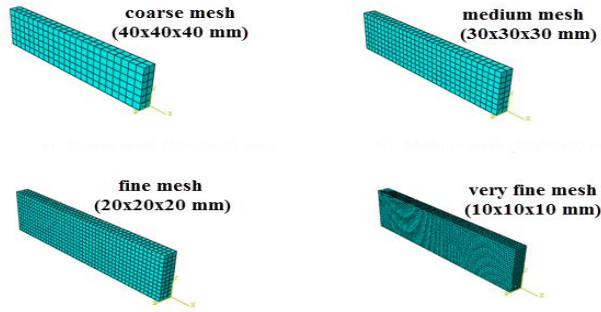
a)   Mesh sizes
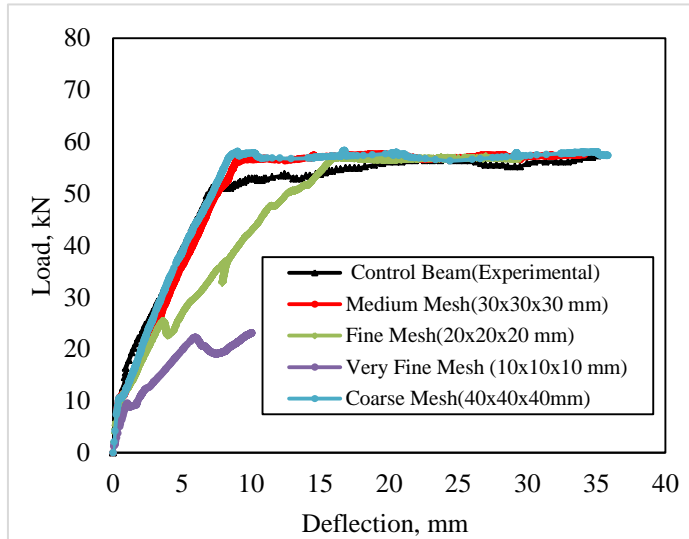
b)   Sensitivity to element size

Figure 5: Various modeling meshes and loading -deflection comparison with mesh sizes

3.4   Nonlinear Solution

In this study, the total deflection applied was divided into a series of deflection increments. Newton method iterations provide convergence, within tolerance limits, at the end of each deflection increment. During concrete cracking, steel yielding and the ultimate stage where a large number of cracks occur, the deflections are applied with gradually smaller increments. Automatic stabilization and small time increment were also used to avoid a diverged solution.

4.0   Nonlinear FE Analysis: Results & Discussion

The present F.E. numerical predictions regarding the failure modes, load versus mid-span deflection, and beams' ductility which were compared and verified with the ones observed experimentally by Choobbor *et al*. (2014). The ratio of experimentally over numerically predicted ultimate flexural capacity and ultimate deflections are listed in Table 5 with values very close to 1.0, which signifies a very good agreement of the numerically predicted values with the respective experimental ones. Moreover, the numerically predicted modes of failure are also in very good agreement with the ones observed during testing. Detailed discussion for these items considered in the present study as follows:

Table 5: Comparison between experimental and finite element results

Specimen	Ultimate load(Pu), kN		Deflection at Pu (δu), mm		Pu_{Exp} / Pu_{EF}	$\delta u_{Exp}/ \delta u_{FE}$
	Exp	FE	Exp	FE		
Control(NS)	57.3	57.48	35.1	34.14	0.99	1.03
C	89.9	90	19.4	19.2	0.99	1.01
CC	98.5	95.5	13	13.2	1.03	0.98
B	73.4	70	22.2	22	1.05	1.01
BB	93	95.9	28	29.14	0.97	0.96
BC	95.8	91.7	16.3	16	1.04	1.02
BCC	101.29	99.5	13	12.9	1.02	1.01
BCB	100.3	99.6	15.8	16.17	1.01	0.98
Mean(M)					1.01	1.00
Coefficient of Variation(COV)					2.73	2.39
Standard Deviation(STD)					0.0276	0.0239
Variance(VAR)					0.00076	0.00057

4.1   Failure Modes

The tested RC beams showed different failure modes including concrete crushing, flexure cracks, debonding of FRP, FRP rupture and concrete cover separation. In FE (ABAQUS) analysis, the maximum principal plastic strain of concrete (PEMAG and PE) is depicted as a means to visualize concrete cracking since no discrete cracks form during the adopted numerical analysis. The control beam failed experimentally and numerically in a typical flexural mode where there was yielding of the flexural steel bars followed by crushing of the concrete at the top face of the beam in the mid-span region, as shown in Figure 6.
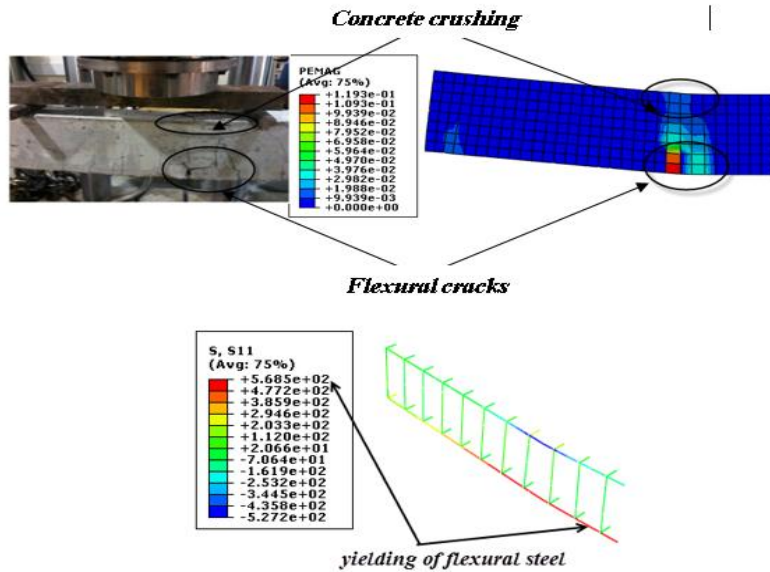
Figure 6: Exp & FE typical flexural failure mode and stress values of reinforcement at failure for control beam (NS)

The BC beam failed by yielding of the steel rebar with major flexural cracks followed by de-bonding of hybrid BC sheet as noted experimentally and modeled numerically as shown in Figure 7.
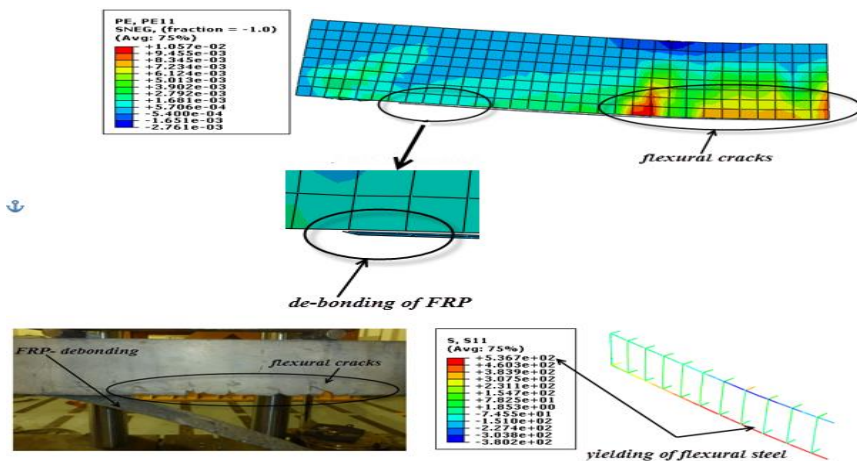
Figure 7: Exp. versus FE of FRP-debonding failure and yielding profile of reinforcement at failure for BC beam

The beams C, CC, BCC, and BCB have nearly the same failure mode; they failed by yielding of the steel rebar followed by FRP delamination (concrete cover separation). The premature debonding failure (concrete cover separation) modes of FRP-strengthened beams, as shown in Figure 8 , is often observed in many experiments as mentioned previously by Zhang *et al*. (2012). In the finite element analysis, the red and green color in the FRP composite sheet indicates sticking of some parts of the concrete cover with it, regarding with blue color, which refers to fully separation of FRP without any remains of concrete cover. Consequently, the present FE model capture accurately the phenomena of concrete cover separation as shown in Figure 8.

Besides, it can be noticed that RC beams strengthened with one layer and two layers of BFRP sheets (Beams B and BB respectively) had the best mode of failure. These beams failed by BFRP sheet rupture, which indicates that the maximum capacity of BFRP sheets was achieved and the strengthening system was fully utilized. Concerning the present FE model, the values of Hashin's tensile strain for BFRP sheet (BB coupon) in most locations along the BB sheet (ranging from 0.67 to0 .061) are bigger than the experimental value of ultimate tensile strain of BB sheet (0.0259, see to Table 4), leading to the complete failure of BFRP sheets, this agree with the experimental shape of failure as shown in Figure 9.

Concerning the three dominant modes of failure(FRP-debonding, FRP- delamination and FRP rupture), the proposed numerical FE analysis can capture these phenomenon accurately compared to the experimental failure shapes as shown in the previous Figures 6,7,8, and 9.
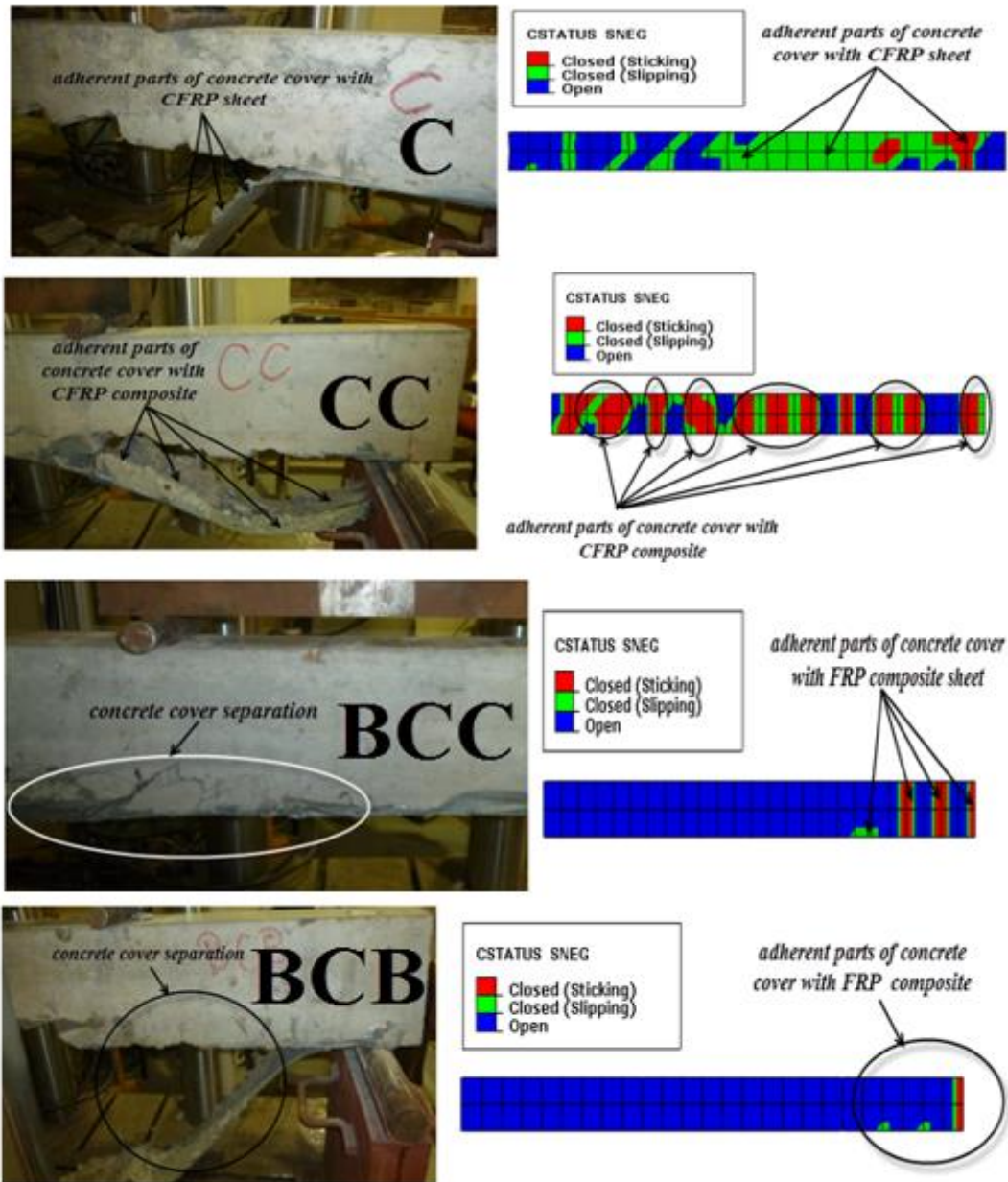
Figure 8: Concrete cover separation failure mode of beams C,CC,BCC, and BCB respectively
(experimentally and numerically)
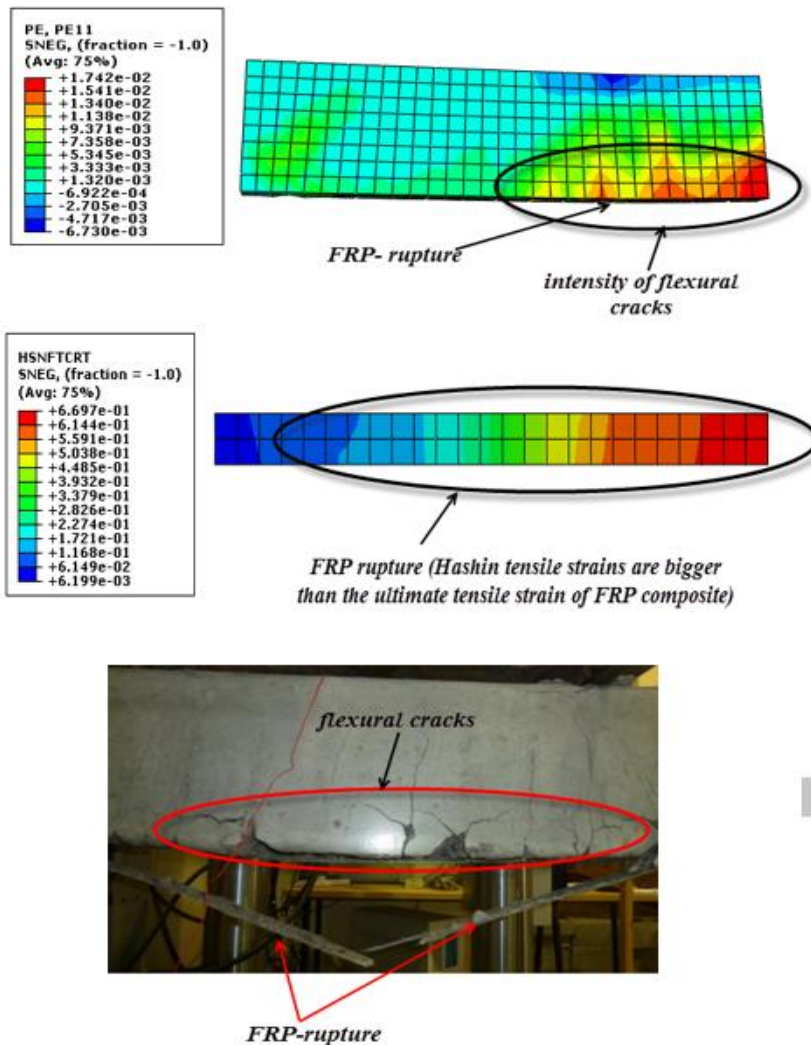
Figure 9: Rupture of BFRP composite sheets of BB beam (experimentally and numerically)

4.2   *Load-Deflection Behaviors*

The observed behavior of the control beam specimen, which were initially tested to obtain the basic structural response of the reinforced concrete rectangular beam specimen without the added complexity of the attached FRP sheets, was, in general, well-predicted by the FE numerical model and also the strengthened ones as can be seen in the Figures from 10 to 17, where the experimental and numerical load–displacement

curves are nearly identical. Table 5 summarizes the results of the experimental testing and the FE analysis for all specimens. The agreement is excellent as attested to by the descriptive statistics (M = 1.01and 1.00, COV = 2.73 and 2.39, STD = 0.0276 and 0.0239, VAR = 0.00076 and 0.00057 concerning ultimate flexural loads and corresponding deflections respectively). Therefore, it was concluded that the developed FE models are valid to predict the response of RC beams strengthened in flexure with externally bonded CFRP sheets, BFRP sheets, and their hybrid combination accurately. The good agreement indicates that the used cohesive model in FE and constitutive models used for concrete, reinforcement, and FRP composites can capture the fracture behavior well. The ultimate load and the maximum deflection of the control beam(NS) specimen is used as benchmark for measuring the performance of other beams as shown in Table 6.
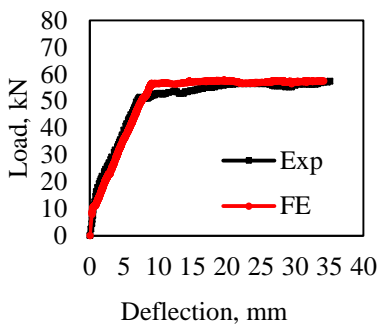
Figure 10: Load-deflection behavior of NS
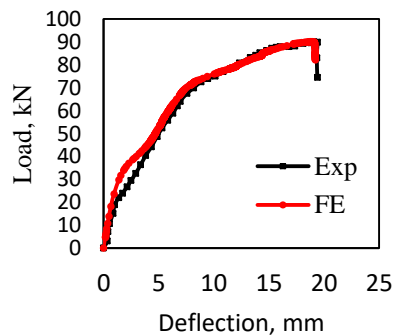
Figure 11: Load-deflection behavior of C
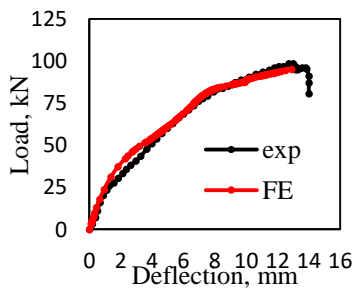
Figure 12: Load-deflection behavior of CC
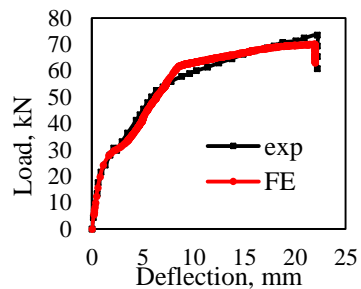
Figure13: Load-deflection behavior of B
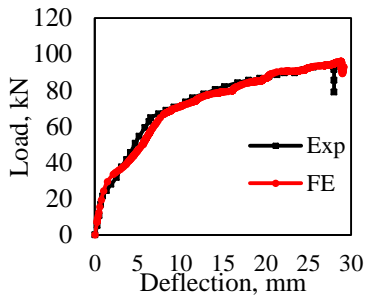
Figure 14: Load-deflection behavior of BB
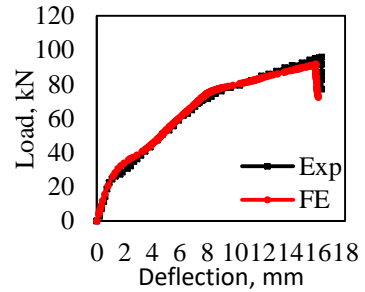
Figure 15: Load-deflection behavior of BC
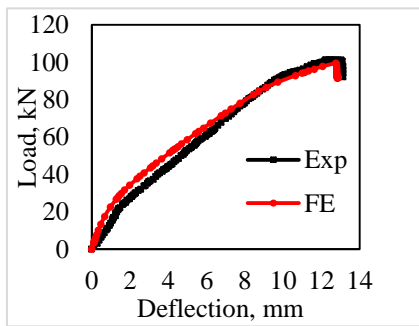
Figure 16: Load-deflection behavior of BCC
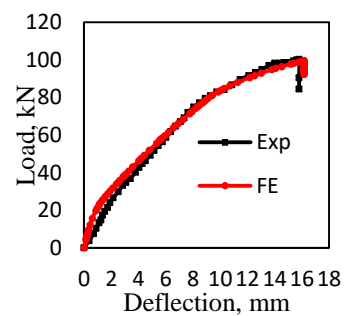
Figure17: Load-deflection behavior of BCB

It is clear from Figures 18, 19 and Table 6 that the strengthened beams have larger post cracking stiffness, higher flexural bearing capacity, and yet lower deflection values than that of the control beam. Figure 20 shows that the increase in the experimental ultimate (peak) load of the strengthened beams ranged from 28% to 77% of the un-strengthened control RC beam (NS). Such increase in the ultimate loads is in agreement with the FE results which ranged from 22% to 73%. It can also be noticed from Figure 20 that BC, BCC and BCB beams which were strengthened with hybrid BFRP and CFRP sheets yielded the highest increase in flexural capacity compared to NS beam (nearly, 73% for experimental results and 70 % for FE ones).

Table 6: Summary of ultimate loads and failure modes

Specimen	Exp		FE		Failure Mode
	P_u	$P_u/P_{u\ NS}$	Pu	$P_u/P_{u\ NS}$	
Control(NS)	57.3	1.00	57.48	1.00	Flexural failure, steel yielding followed by concrete crushing
C	89.9	1.57	90	1.56	Steel yielding followed by FRP delamination (concrete cover separation)
CC	98.5	1.72	95.5	1.66	Steel yielding followed by FRP delamination (concrete cover separation)
B	73.4	1.28	70	1.22	Steel yielding followed by FRP rupture
BB	93	1.62	95.9	1.67	Steel yielding followed by FRP rupture and concrete crushing at loading support
BC	95.8	1.67	91.7	1.59	Steel yielding with major flexural cracks followed by FRP -debonding
BCC	101.29	1.77	99.5	1.73	Steel yielding followed by FRP delamination (concrete cover separation)
BCB	100.3	1.75	99.6	1.73	Steel yielding followed by FRP delamination (concrete cover separation)
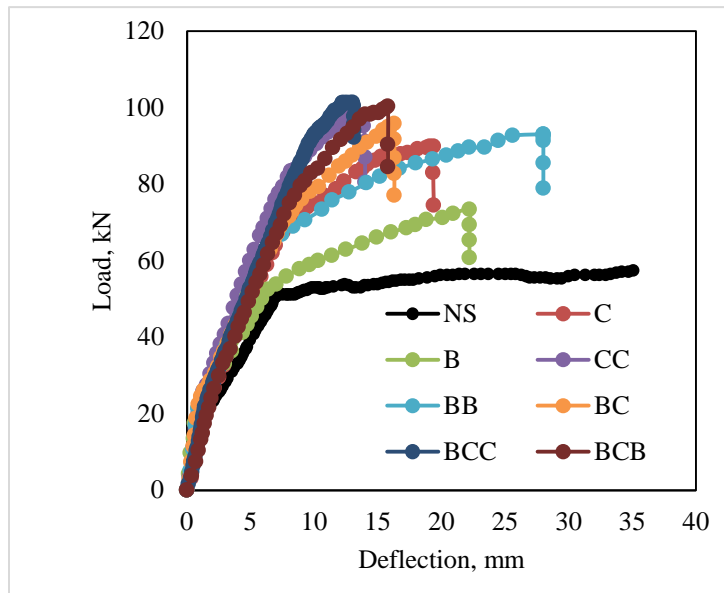
Figure18: Experimental load-deflection curves of all tested beams
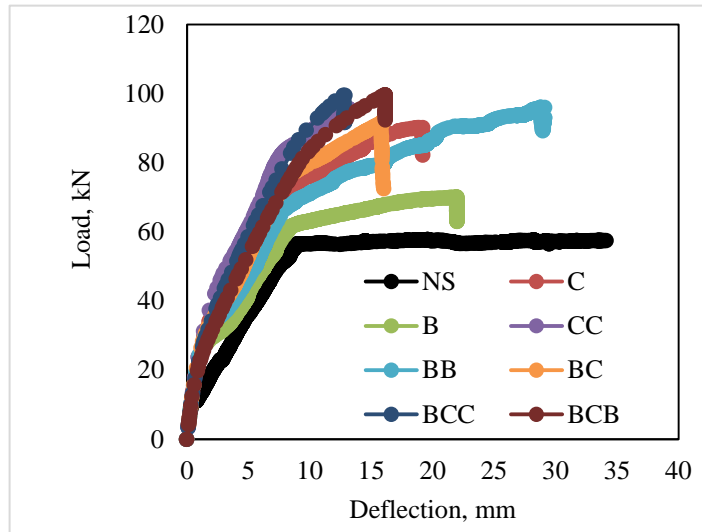
Figure 19: Numerical load-deflection curves of all tested beams
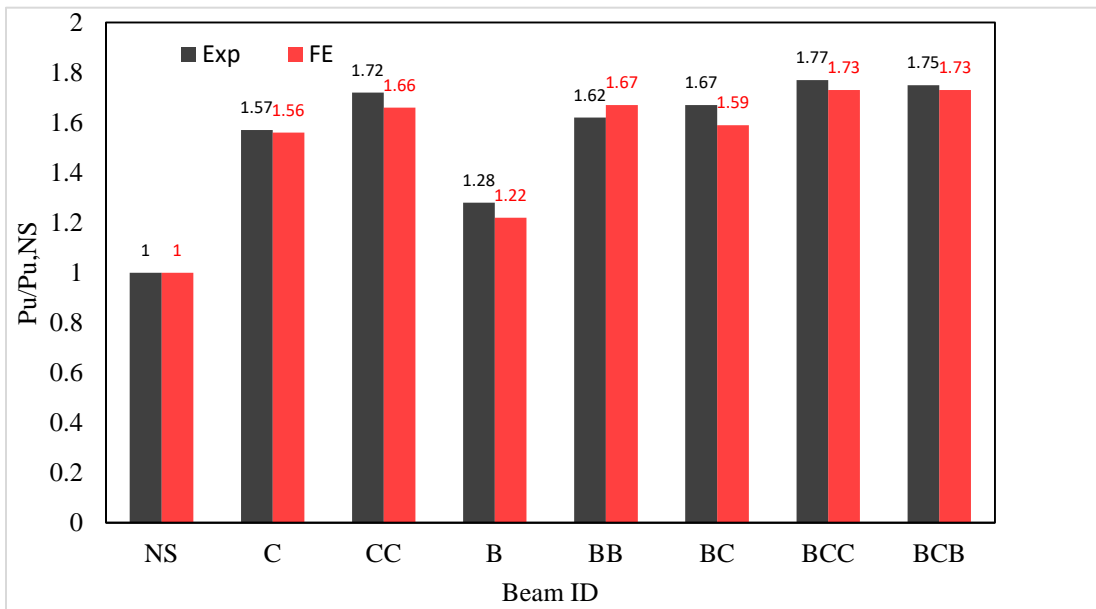
Figure 20: Exp. & FE ultimate flexural capacity of all tested beams related to control one

4.3   Ductility

The ductility of a beam can be defined as its ability to sustain inelastic deformation without loss in load carrying capacity, prior to failure. Ductility can be defined in terms of deformation or energy. In the case of steel-reinforced beams, where there is clear plastic deformation of steel at yield, ductility can be calculated using deformation methods. It can be defined as the ratio of ultimate deformation to the deformation at yield. The deformations can be strains, deflections, or curvatures. In the case of beams strengthened with FRP, there is usually no clear yield point; therefore, the classical definition of ductility is not applicable. Therefore, ACI 440.1R-06 (2006) reported that the ductility of the FRP reinforced beams can be evaluated by means of the deformability factor (D_F), defined as the ratio of the energy absorption at ultimate (area under load-deflection curve up to ultimate load) to the energy absorption at service load (at the serviceability deflection limit of span / 180).

It can be noticed from Table 7 that the deformability factors (DF), based on experimental results are agree well with ones, which predicted from the finite element models. Beams strengthened with various FRP-composite sheets exhibited 10% to 67% lower ductility than that of the un-strengthened beam, and 9% to 71% lower ductility than that of the un-strengthened beam for both experimental and FE results respectively. The beam strengthened with two layers on BFRP sheets (BB) had the highest ductility among all strengthened beams with 10% only reduction in RC beam ductility compared to the un-strengthened beam.CSA-S6-00(2000) specified that D_F must be more than 4 to ensure a ductile failure. Whereas, most of the strengthened beams failed in brittle mode due to concrete cover separation, they have D_F under this limit as shown in Figure 21. Consequently, it is very important to check the deformability in design of FRP-strengthened beams.

Table 7 : Summary of ductility (deformability factors) results

Beam ID	Experimental Results			Finite Element Results(ABAQUS)		
	D_F	$D_F/D_{F,NS}$	% decrease	D_F	$D_F/D_{F,NS}$	% decrease
NS	5.2	1	0	5.4	1	0
C	2.9	0.56	44	2.7	0.50	50
CC	1.76	0.34	66	1.6	0.30	70
B	3.1	0.60	40	3.2	0.59	41
BB	4.66	0.90	10	4.9	0.91	9
BC	2.2	0.42	58	2.16	0.40	60
BCC	1.73	0.33	67	1.56	0.29	71
BCB	2.2	0.42	58	2.33	0.43	57
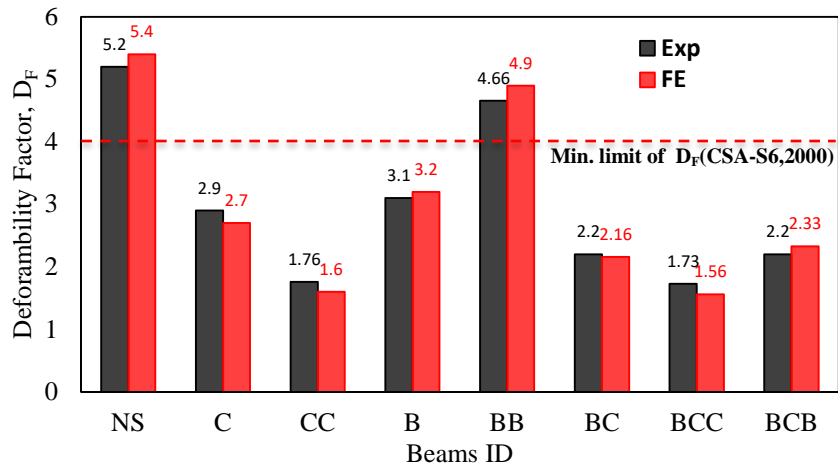
Figure 21: Experimental and finite element results of ductility of all beams

4.4   Hybrid Effect of CFRP and BFRP

The effect of combining CFRP and BFRP sheets in strengthening of concrete beams is illustrated experimentally and numerically in Figures 20 and 21 . The two figures compare the ultimate flexural capacity and ductility of the all studied beams. It can be noticed that the beam strengthened with two layers of CFRP sheet (CC) presented the highest flexural capacity and the lowest ductility. In contrast, the RC beam strengthened with two layers of BFRP sheet (BB) showed the highest ductility and the lowest flexural capacity. On the other hand, the beam which was strengthened with the hybrid combination of CFRP and BFRP sheets, for two layers of FRP-composites (one layer of BFRP and one layer of CFRP) as the BC beam which presented higher flexural capacity than the beam strengthened with two layers of BFRP (BB) and higher ductility than the beam strengthened with two layers of CFRP (CC). Similarly, for strengthening by the three composites layers, as BCB beam attained higher flexural capacity nearly the same as BCC with higher ductility than it.

Concluded from the above, that the hybrid combination of CFRP and BFRP sheets provides an enhanced strengthening system, where it combines the high strength of CFRP sheets and the high ductility of BFRP sheets as BC and BCB beams. In addition, the best hybrid combination of CFRP and BFRP sheets is realized by BCB beam, because it gives highest flexural capacity and ductility simultaneously compared with other beams that strengthened with other combinations.

5.0   New Approach to Improve the Performance of Hybrid FRP-Strengthened Beams

This section is finite element study was prepared to prevent as possible the concrete cover separation phenomenon (FRP delamination) which repeated   during failure of most hybrid FRP-strengthened beams (Choobbor *et al.*, 2014). The major goal of this analysis is introduce a new retrofitting method, which utilize hybrid FRP-composite to their full capacity as much as possible, leading to rupture of the hybrid FRP-composite instead of concrete cover separation at failure. To achieve this target, a new technique was evaluated numerically by replacing of existing concrete cover to high strength one. In many cases of retrofitting of concrete beams, the concrete cover was nearly damaged due to many reasons, including: reinforcement corrosion especially in marine environment, fire exposure, aggressive chemical attack, etc. Removing of the deteriorated concrete cover and replacing by other new high strength one is usually done by shotcrete before installation of FRP sheets. In this section, the replacement of concrete cover was studied numerically by nonlinear finite element analysis.   The concrete cover of BCB beam was replaced by others with high strength concretes which have various grades (f_c ranging from 20 to 200 MPa).

Figures 22 and 23 shows that increase of cover strength from 40 to 150 MPa for example, leads to a marked increase in flexural capacity of BCB beam equals 14% and at the same time slightly decrease in the ductility equals 5.8%. Figures 24 and 25 shows the finite element results of rupture stain of BCB sheet expressed by Hashin's tensile strain, it is clear that, above 50 MPa of compressive strength of concrete cover, the dominate failure mode is BCB rupture (no cover separation was noticed), because all values of ultimate rupture stain of BCB sheets which were bonded with concrete cover (which have strength more than 50 MPa) are bigger than the experimental ultimate tensile strain of BCB (0.0208, see Table 4). The FE results show that concrete cover replacement with HSC provided better flexural capacity and failure mode; beams failed by BCB sheet rupture rather than concrete cover separation. This means that the optimum capacity of BCB sheet was achieved in strengthening operation, this agrees with the studies which were carried out by Al-Saidy *et al*. (2009) and Ray *et al*. (2010).
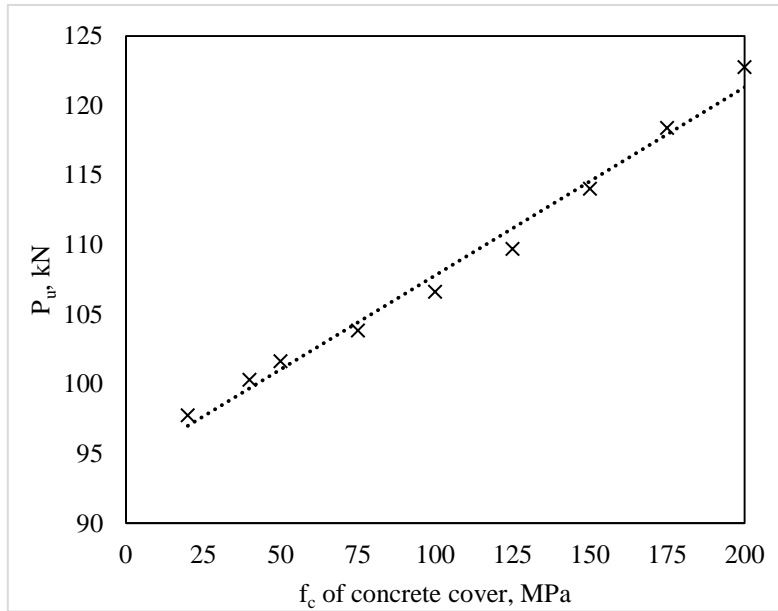
Figure 22: Effect of concrete strength of cover upon flexural capacity of BCB beam
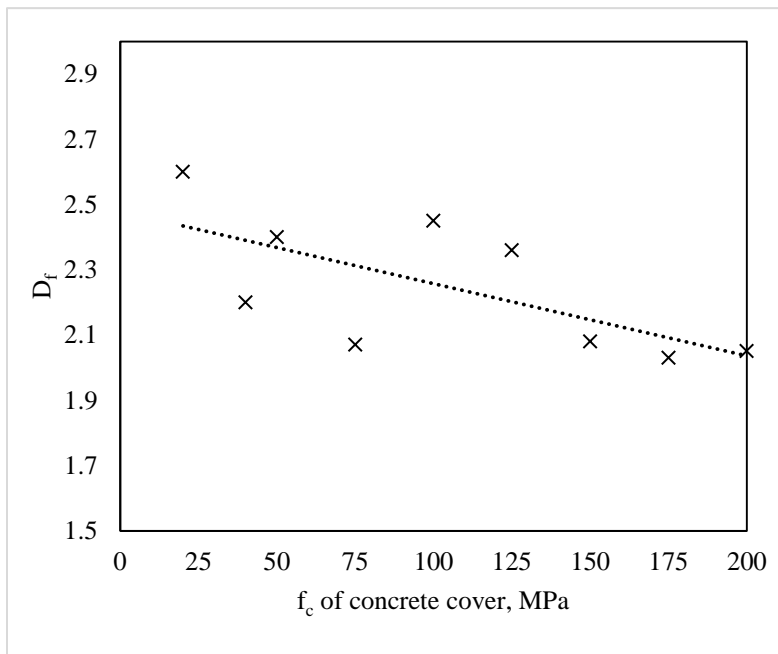
Figure 23: Effect of concrete strength of cover upon ductility of BCB beam
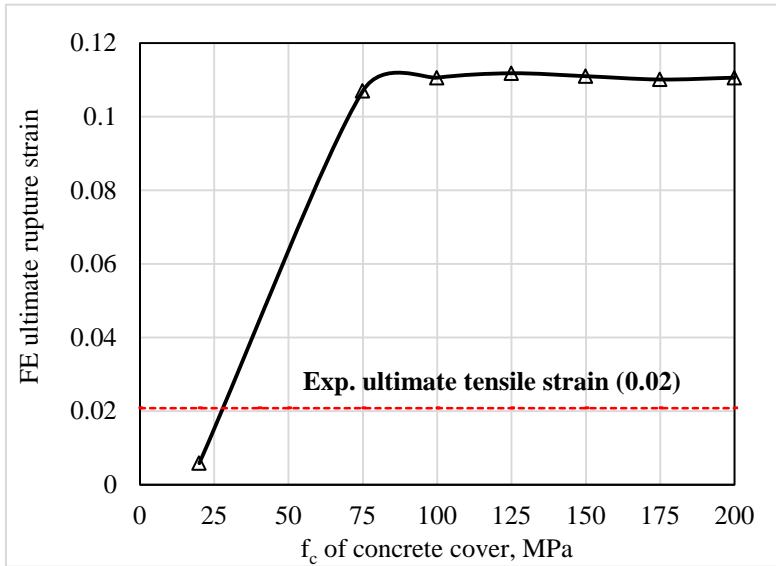
Figure 24: Effect of Concrete strength of cover upon the rupture strain of BCB sheet

Rupture of BCB sheet
Hashin tensile strains are bigger than the
ultimate tensile stain(0.0208)
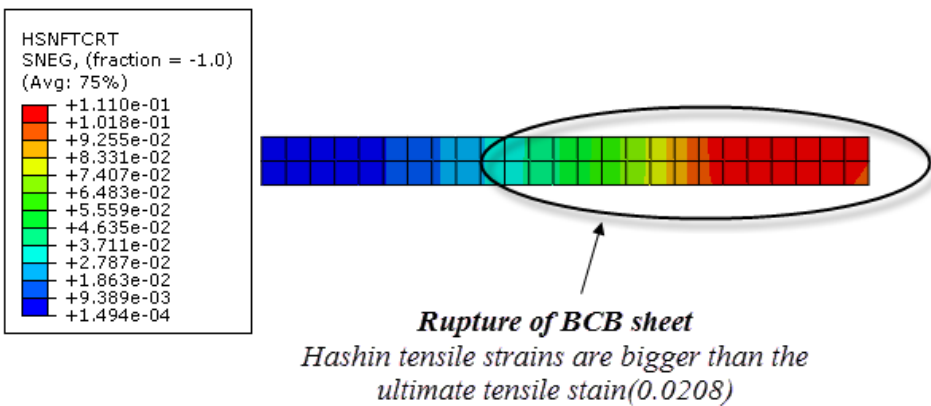
Figure 25: FE rupture stain of BCB sheet that bonded with 150MPa concrete cover

6.0   Conclusions

The behavior of reinforced concrete beams externally strengthened with CFRP sheets, BFRP sheets, and their hybrid combination (CFRP-BFRP) was simulated using the finite-element method (FEM). The developed FE model has been validated by comparing the predicted results to the experimental data. Conclusions derived from this study are as follows:

1. Nonlinear finite element analysis accounting a proper constitutive model and takes into account the materials nonlinearity of cracked concrete, steel bars, epoxy and FRP can predict correctly the behavior of FRP-strengthened concrete beams. Such numerical models are very important and indispensable to well understand the complex non-linear mechanisms such as the cracking and crushing of concrete, and the debonding and fracture of the FRP sheets that are extremely difficult to assess experimentally.

2. Including the FRP-concrete interface (surface-based cohesive behavior based on a traction-separation law) in the numerical model can capture the real behavior of the FRP-strengthened beams under the increasing flexural load. The successful FE models, accurately capturing the basic structural response in terms of ultimate load, failure modes and overall load–displacement response.

3. This study proven numerically and verified experimentally that the, hybrid combination of CFRP and BFRP sheets provides an enhanced strengthening system, where it combines the high strength of CFRP sheets and the high ductility of BFRP sheets as BC and BCB beams. In addition, the best hybrid combination of CFRP and BFRP sheets is realized by BCB beam, because it gives highest flexural capacity and ductility simultaneously compared with other beams that strengthened with other combinations.

4. From this study, FRP-strengthened concrete beams failed in brittle mode, have deformability factors less than a minimum value of four. Therefore, it is strongly recommended to check the deformability with taking higher factor of safety in design of FRP-strengthened concrete beams.

5. The retrofitted RC beams fail before the hybrid FRP sheets reach failure point. This limits the strengthening effect of the hybrid FRPs. This paper introduces the effective solution to overcome this problem numerically, by replacing the concrete in the cover zone with new layer of high strength concrete prior to strengthening with FRP which was found to be more effective in the load transfer mechanism between the FRP and concrete leading to utilize of the full capacity of hybrid FRP-composites.

6. More research work (experimentally and numerically) is needed to verify the proposed approach in this study, concerning how to completely utilize of the full capacity of hybrid FRP-composites in strengthening of concrete beams and preventing the concrete cover separation phenomenon (FRP delamination)   , by replacing the old concrete cover with very efficient repairing materials as ultra-high-performance-fiber reinforced concrete (UHPFRC). Especially, it has numerous advantages over other concretes as higher compressive and tensile strength, ductility, bonding strength and durability as reported by Toutlemonde and Resplendino (2011).

References

ABAQUS/Standard (2016). ABAQUS standard user's manual, Dassault Systèmes Simulia Corp., Pawtucket (RI, USA): Hibbitt Karlsson & Sorensen Inc.; USA.

ACI 318(2014). ACI Committee *Building Code Requirements for Structural Concrete and Commentary*. American Concrete Institute. Farmington Hills. Michigan. USA.

ACI 440.1R (2006). ACI Committee *Guide for the Design and Construction of Concrete Reinforced with FRP Bars*. American Concrete Institute. Farmington Hills. Michigan. USA.

Ahmad, E. and Sobuz, H. (2011). *Flexural Performance of CFRP Strengthened RC Beams with Different Degrees of Strengthening Schemes*. International Physical Sciences 6: 2229–2238.

Al-Saidy, A., Al-Harthy, A. and   Al-Jabri, K.(2009). *Effect of damaged concrete cover on the structural performance of CFRP strengthened corroded concrete beams*. Concrete Repair. Rehabilitation and Retrofitting II Conference. London.

Ashour,A.,   El-refaie, S. and Garrity, S.(2004). *Flexural Strengthening of RC Continuous Beams Using CFRP Laminates*. Cement and Concrete Composites 26: 765–775.

Choi, D., Kang,T.,   Ha,S., Kim,K., and Kim, W.(2011). *Flexural and bond behavior of concrete beams strengthened with hybrid carbon-glass fiber-reinforced polymer sheets*. ACI Structural Journal 108: 90-98.

Choobbor, S, Hawileh, R and Hawileh, R. (2014). *Performance of reinforced concrete beams externally strengthened with Carbon and Basalt Sheets*. International Conference on Infrastructure Management. Assessment and Rehabilitation Techniques. Sharjah.

CSA-S6-00 (2000). *Canadian Highway Bridge Design Code*. Canadian Standards Association. Rexdale. Canada.

Grace,N., Abdel-Sayed,G., and Ragheb,W.(2002). *Strengthening of concrete beams using innovative ductile fiber-reinforced polymer fabric*. ACI Structural Journal 99: 692-700.

Hawileh,R., Rasheed, H., Abdalla, J. and Al-Tamimi, A.(2014).*Behavior of reinforced concrete beams strengthened with externally bonded hybrid fiber reinforced polymer systems*. Materials and Design 53: 972–982.

Hillerborg, A.,(1985). *The Theoretical Basis of a Method to Determine the Fracture Energy G_f of Concrete*. Materilas and Structures 108:

Kim,H., and Shin, Y.(2011). *Flexural behavior of reinforced concrete (RC) beams retrofitted with hybrid fiber reinforced polymers (FRPs) under sustaining loads*. Composite Structures 93: 802-811.

Obaidat Y.T.,(2011). *Structural Retrofitting of Concrete Beams Using FRP - Debonding Issues*. Ph.D. Dissertation. Lund University.Sweden.

Obaidat Y.T., Heyden S., and Dahlblom O.(2010). *The effect of CFRP and FRP/concrete interface models when modelling retrofitted RC beams with FEM*. Composite Structures 92: 1391-1398.

Ray, I., Parish, G., Davalos, J., and Chen. A.(2010). *Effect of Concrete Substrate Repair Methods for Beams Aged by Accelerated Corrosion and Strengthened with CFRP*. Journal of Aerospace Engineering 24: 227-239.

Saenz, LP.(1964). *Discussion of Equation for the stress-strain curve of concrete*. ACI Journal 61: 1229–1235.

Sveinsdóttir, S. (2012). *Experimental research on strengthening of concrete beams by the use of epoxy adhesive and cement-based bonding material*. M.Sc. Dissertation. Reykjavík University. Iceland.

Toutlemonde, F. and Resplendino, J. (2011). *Designing and Building with UHPFRC: State of the Art and DevelopmentBook*. John Wiley & Sons Inc.

Wu,Z., Li, W., and Sakuma, N.(2006). *Innovative externally bonded FRP/concrete hybrid flexural members*. Composite Structures72: 289-300.

Xiong,G., Yang, J. and Ji,Z.(2004). *Behavior of reinforced concrete beams strengthened with externally bonded hybrid carbon fiber- glass fiber sheets*. Composites for Construction 8 : 275-278.

Zhang, D., Ueda, T., and Furuuch, H.(2012). *A New Analytical Model for Concrete Cover Separation of R/C Beams Strengthened with FRP Laminates*. The Third Asia-Pacific Conference on FRP in Structures, Japan.